WASHINGTON STATE DEPARTMENT OF
Natural Resources
Jennifer M. Belcher - Commissioner of Public Lands

Produced in cooperation with the U.S. Geological Survey
National Cooperative Geologic Mapping Program
Agreement Number 99HQAG0136

WASHINGTON DIVISION OF GEOLOGY AND EARTH RESOURCES
Raymond Lasmanis, State Geologist

PLATE 4

OPEN FILE REPORT 2000-6
GEOLOGIC MAP OF THE ANACORTES SOUTH AND
LA CONNER 7.5-MINUTE QUADRANGLES,
WESTERN SKAGIT COUNTY, WASHINGTON

BEDROCK STEREONET DIAGRAMS

Stereonet diagrams for the Fidalgo Complex (FC) and the Goat Island terrane (GIT). The stereonet counting method is Gaussian, smoothed (K=100). The contour intervals are 0, 2, 4, 6.....18 percent data/ 1 percent area. All nets have unweighted analyses. Much of our structural data is plotted on Plate 1 and this plate (Maps A and B). However, in many areas only the most representative structural data is plotted due to the map scale. The structural data set also includes data from directly adjacent areas (for example, Deception Pass, Crescent Harbor, and Utsalady 7.5-minute quadrangles) which are not represented on our maps. For example, very little of the GIT data obtained from the Martha's Bay area directly south of the Anacortes South quadrangle is shown on the maps. Structural symbol numbers referred to in the stereonet captions refer to the numbers adjacent to the structural symbols under the map explanation (Plate 1).

The FC records two main deformational episodes. D1 is a heterogeneous and locally penetrative thrust deformation dated as mid-Cretaceous by Brandon and others (1988) elsewhere in the San Juan Islands. D2 is a later high-angle fault episode that is probably mostly Tertiary. The D1 semi-penetrative to penetrative structural features in the FC (for example, S1 cleavage and L1 stretching lineations) are only locally observed and are characteristically found in geologic units of relatively low competence (for example, medisedimentary sequences containing significant metasiltstones or meta-argillite). Initial shortening is accomplished throughout much of the stratigraphic sequence by intraformational folding. Further strain and thrust yielding is progressively concentrated into narrowing zones that approximate simple shear and utilize incompetent lithologies (for example, thick metasedimentary sequences). Thus, the deformation is hetero-geneous, and metasedimentary lithologic packages bear much of the semi-penetrative to penetrative deformation, particularly near thrusts.

Penetrative deformation of metasedimentary rocks of the GIT is much more pervasive. Furthermore, the GIT metasediments contain F1, F2, and F3 folds that record two, possibly three, deformational episodes. Thrust deformational fabric sand structures in the FC may be locally present within the GIT. The structural complexity of the GIT is at least partially the result of it's location within the Darrington-Devils Mountain fault zone (DDMFZ) in the southernmost portion of the study area (Plate 1). The DDMFZ is an active strike-slip zone (Johnson and others, in progress) in which deformation began in the Tertiary, perhaps as early as the mid-Cretaceous. (An expanded discussion of the structural history of the study area will appear in a future publication.)

FIDALGO COMPLEX

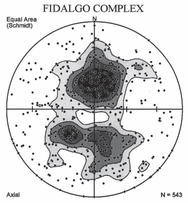

Net 4.1. All bedding in the FC. (Poles to bedding.) Includes structure symbols 1, 2, and 4 (Plate 1). Note the high density of bedding orientations with a shallow southerly dip. Bedding planes of this orientation are common in deformational zones of moderate to high semi-penetrative to penetrative thrust shear. Scatter in bedding orientations is mostly the result of the variation in D1 thrust shear strain. (See Nets 4.17-4.20 for high-strain deformational fabrics in the FC, including the orientation of overturned bedding.)

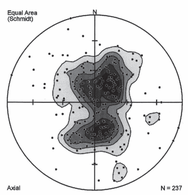

Net 4.3. All S1 foliation in the FC. (Poles to foliation.) Includes structure symbols 7-16 (Plate 1). Also includes minor Reidel fracture data. Note the high density of foliation orientations with subhorizontal to shallow southerly dip. Fabric is probably the result of heterogeneously distributed thrust shear in the FC. S1 foliation locally contains an L1 stretching lineation (Net 4.9) and is axial planar to F1 folds of bedding (for example, Nets 4.1 and 4.17-4.20). Scatter in foliation orientations is mostly the result of the variation in D1 thrust shear strain. (See Nets 4.17-4.20 for high-strain deformational fabrics in the FC.)

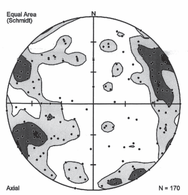

Net 4.5. All post-metamorphic prominent outcrop-scale fractures and faults in the FC. (Poles to fractures and faults.) Includes structure symbols 21-24 (Plate 1). Many faults and fracture planes contain slickenlines or striations (Net 4.7). Although much scatter exists, many moderate to steeply dipping fracture planes indicate high-angle, northwest- and northeast-striking faults.

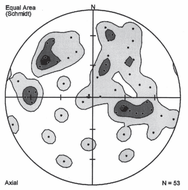

Net 4.7. All post-metamorphic slickenlines (including striations) in the FC. Includes structure symbols 27 and 28 (Plate 1). Many slickenlines on faults and fractures (Net 4.5) indicate oblique, high-angle faulting in the FC. Some northeast-striking faults appear to record largely strike-slip offset.

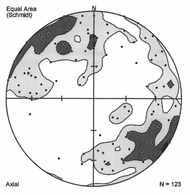

Net 4.9. All undifferentiated L1 lineations, including stretching lineations, in the FC. Includes structure symbols 29-34 (Plate 1). Tectonic lineations reflect north-south compression (probably intraformational thrust deformation). Most lineations shown are stretching lineations. These lineations occur on S1 foliations, including a semi-penetrative to penetrative cleavage (Net 4.3). S1 foliation is locally axial planar to F1 folds of bedding (for example, Nets 4.1 and 4.17-4.20).

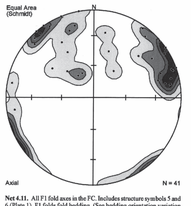

Net 4.11. All F1 fold axes in the FC. Includes structure symbols 5 and 6 (Plate 1). F1 folds fold bedding. (See bedding orientation variation in Nets 4.1, 4.19, and 4.20.) F1 folds typically trend shallowly to the northeast. Most F1 folds are overturned and contain a shallowly dipping S1 axial planar cleavage (Nets 4.3 and 4.17). Outcrop F1 folds are interpreted to mimic large overturned folds in the FC as a result of D1 thrusting (Plate 2, cross sections E-E' and F-F').

GOAT ISLAND TERRANE

Net 4.2. All bedding in the GIT. (Poles to bedding.) Includes structure symbols 1 and 2 (Plate 1). Note the folding of bedding around shallowly plunging, mostly east-trending axes (Net 4.12). GIT bedding is subparallel to the GIT S1 cleavage (Net 4.4). GIT bedding is transposed subparallel to the S1 cleavage in metasedimentary rocks as evidenced by rarely observed F1 folds of bedding.

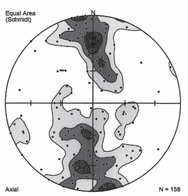

Net 4.4. All S1 cleavage in the GIT. (Poles to bedding.) Includes structure symbols 7 and 8 (Plate 1). GIT cleavage is subparallel to the GIT bedding. (See Net 4.2.) Note the folding of cleavage around shallowly plunging, east-west-trending axes. (Also see Nets 4.12 and 4.16.) The S1 foliation locally contains two probable stretching lineations (Net 4.10) indicating a complex deformational history.

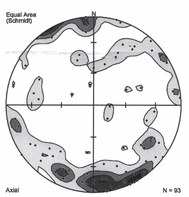

Net 4.6. All post-metamorphic prominent outcrop-scale fractures and faults in the GIT. (Poles to fractures and faults.) Includes structure symbols 21-24 (Plate 1). Faults and striated fracture plane orientations indicate high-angle, largely west-striking faulting within the DDMFZ (Plate 1). Many fault and fracture planes contain slickenlines or striations (Net 4.8).

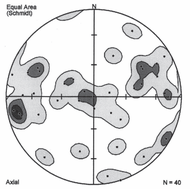

Net 4.8. All post-metamorphic slickenlines (including striations) in the GIT. Includes structure symbols 27 and 28 (Plate 1). Slickenlines occur mostly on high-angle faults and fractures (see Nat 4.6). Measured faults and striated fracture planes reflect high-angle, east-west-striking fault and fracture planes within the broad DDMFZ (Plate 1). (Compare slickenline orientations with stretching lineations within the GIT [Net 4.10].)

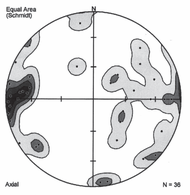

Net 4.10. Stretching lineations in the GIT. Includes structure symbols 29-34 (Plate 1). Stretching lineations in the GIT show two maxima: a predominant shallowly east-west-plunging maximum subparallel to the strike of the DDMFZ and a locally observed, shallowly NNW-SSE-plunging stretching lineation subparallel to the L1 lineations in the FC. GIT stretching lineations occur on a penetrative S1 cleavage (Net 4.4).

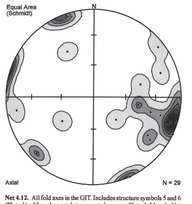

Net 4.12. All fold axes in the GIT. Includes structure symbols 5 and 6 (Plate 1), although most data are not shown on Plate 4, Map A. Net contains a composite of F1 (rare), F2 (local), and F3 (pervasive) fold axes. GIT folds of all generations very typically plunge shallowly to the east. Fold axes shown include rare F1 folds of bedding, overturned and tight to isoclinal F2 folds of the S1 cleavage, and the open and upright F3 folds (Net 4.16). A few of the late F3 folds are kink folds. Late F3 folds result in the broad folding of cleavage (and the subparallel bedding) along a shallowly plunging east-west trend (Nets 4.2 and 4.4). The late F3 folding is predominantly Tertiary and related to transpressional offset along the DDMFZ.

FIDALGO COMPLEX

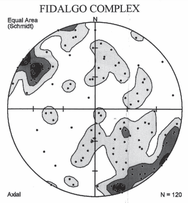

Net 4.13. Syn-metamorphic veins in the FC obtained from outcrops containing D1 fabrics (for example, S1 foliations or fractures). (Poles to veins.) Includes structure symbols 25 and 26 (Plate 1). Veins are complexly oriented and probably the result of several deformational episodes. However, veins found in D1 fabrics are typically subperpendicular to the L1 stretching lineation (Net 4.9) and are probably the result of an east-trending thrust shear deformation. The dominant northeast-southwest strike of the veins suggests mostly northwest-southeast extension subparallel to L1 (Net 4.9).

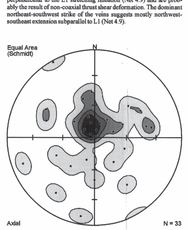

Net 4.15. F1 axial planes in the FC. (Poles to axial planes.) Includes structure symbols 11-15 (Plate 1). F1 folds of bedding very typically contain an axial planar S1 cleavage (Net 4.3). In areas of high D1 strain, the axial planar S1 cleavage typically dips very shallowly to the south (Net 4.17) and bisects the limbs of folded bedding (Nets 4.19 and 4.20).

GOAT ISLAND TERRANE

Net 4.14. Syn-metamorphic veins in the GIT. (Poles to veins.) Includes structure symbols 25 and 26 (Plate 1). Veins are complexly oriented and the result of several deformational episodes. However, veins found in GIT fabrics are subperpendicular to both the east-west and NNW-SSE stretching lineation maxima (Net 4.10) and are probably the result of at least two deformational episodes. The timing and kinematics of D1 are poorly constrained and may be related to early movement on the DDMFZ and (or) syn-metamorphic thrust deformation.

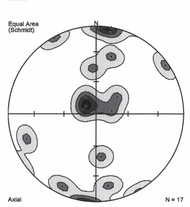

Net 4.16. Fold axial planes in the GIT. (Poles to axial planes.) S1 cleavage is axial planar to F1 folds of bedding in the GIT. Other axial plane information not represented on Map A (this plate). GIT F1, F2, and F3 folds very typically plunge shallowly to the east (Net 4.12). Folds include rarely observed F1 folds of bedding, overturned and tight to isoclinal F2 folds of the S1 cleavage (typically shallowly dipping axial planes on the stereonet), and the open upright F3 folds of cleavage (typically steeply dipping axial planes on the stereonet). F2 folds are only locally observed. Late F3 folds result in the broad folding of cleavage (and the subparallel bedding) along a shallowly plunging east-west trend (Nets 4.2 and 4.4).

Relatively High-Strain Deformational Fabrics

Stereonet diagrams showing some of the relatively high-strain metamorphic fabrics and structural features in the Fidalgo Complex (FC). (See D1 discussion above.) Note the shallowly south dipping maxima for the various high-strain, planar structural features in the FC. D1 thrusting resulted partial transposition (sub-parallelism) of the bedding (both upright and overturned) in zones of relatively high strain. The sub-parallelism of these planar structures is interpreted to be the result of D1 north- to northwest- directed thrusting and associated semi-ductile to ductile thrust deformation. North to northwest vergence is implied by the L1 tectonic lineations (Net 3.9), S1 semi-penetrative to penetrative cleavage and Reidel fractures (Nets 3.3 and 4.17), mostly overturned F1 fold axes (Net 3.11), and extensional veins (Net 4.13).

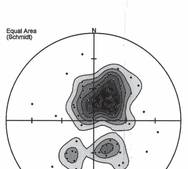

Net 4.17. High- to very high-strain S1 foliations and fractures in the FC. Data from sites containing moderately to very well-foliated rocks. (Poles to foliation.) Includes structure symbols 7-16 (Plate 1). Note the high density of foliation orientations with subhorizontal to shallow southerly dip. Fabric is probably the result of distributed thrust shear in the FC. S1 foliation locally contains an L1 stretching lineation (Net 4.9) and is locally axial planar to F1 folds of bedding (for example, Nets 4.1, 4.17-4.20).

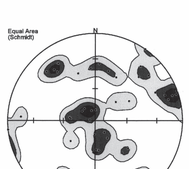

Net 4.18. Selected Reidel fracture planes and thin protomylonitic shear zones near thrusts in the FC. (Poles to fractures.) Includes structure symbols 9, 10, and 16 (Plate 1). Fracture analyses at sites near thrusts show interopeging Reidel fracture patterns with P shear zones and subsidiary Y, R, and R' fracture planes. Striated fracture planes commonly contain striations that plunge shallowly northwest or southeast, subparallel to nearby stretching lineations in moderately to well-cleaved rocks.

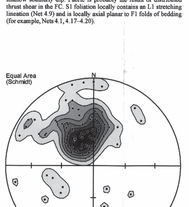

Net 4.19. Overturned bedding in the FC. (Poles to bedding.) Includes structure symbol 4 (Plate 1). (Bedding top indicators are ambiguous at many FC sites.) Overturned bedding shown an overall moderately steep to shallow southerly dip. As shown on Plate 2 (cross section E–E', south Similk Bay), well-displayed overturned bedding consistently dips more steeply than the axial planar S1 cleavage dips to nonvocale asymmetric F1 folds prominent in this area, indicating that the area resides on the limb of a larger fold. The axial planar S1 foliation (Nets 4.3 and 4.17) locally contains an L1 stretching lineation (Net 4.9) and is locally axial planar to F1 folds of bedding (for example, Net 4.20). Beddings of this orientation are common in deformational zones of moderate to high semi-penetrative to penetrative thrust shear.

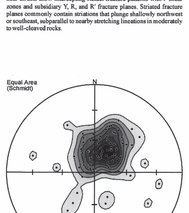

Net 4.20. FC bedding in high- to very high-strain areas containing moderately to very well-foliated rocks. (Poles to bedding.) Includes structure symbols 1, 2, and 4 (Plate 1). Note the similar orientation of FC overturned bedding (Net 4.19) and S1 foliation (Net 4.17). S1 foliation locally contains an L1 stretching lineation (Net 4.9) and is axial planar to locally observed F1 folds of bedding (for example, Nets 4.1, 4.11, and 4.17). The D1 fabric is probably the result of distributed or heterogeneous thrust shear in the FC.

MAP A

Representative foliation, lineation, and fracture structural data for bedrock in the Anacortes South quadrangle and southeastern corner of the La Conner 7.5-minute quadrangle. See Plate 1 for the geologic map and bedding orientations and Plate 3 for the explanational structure symbols and additional stereonets.

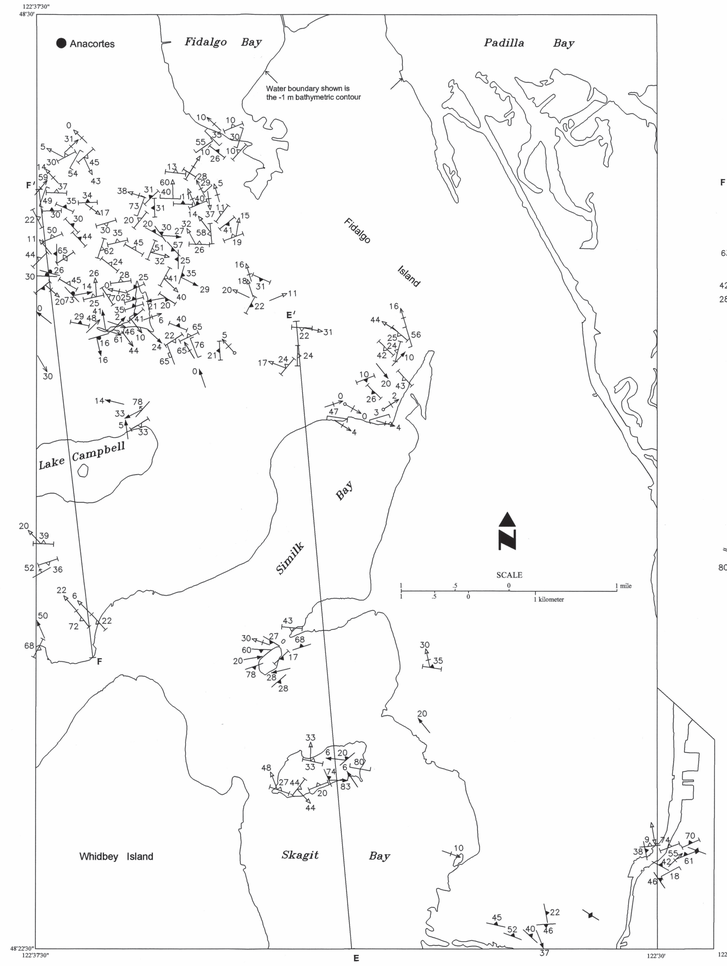

MAP B

Representative fault, fracture, joint, and vein data for bedrock in the Anacortes South quadrangle and southeastern corner of the La Conner 7.5-minute quadrangles. See Plate 1 for the geologic map and bedding orientations and Plate 3 for the explanational structure symbols and additional stereonets.

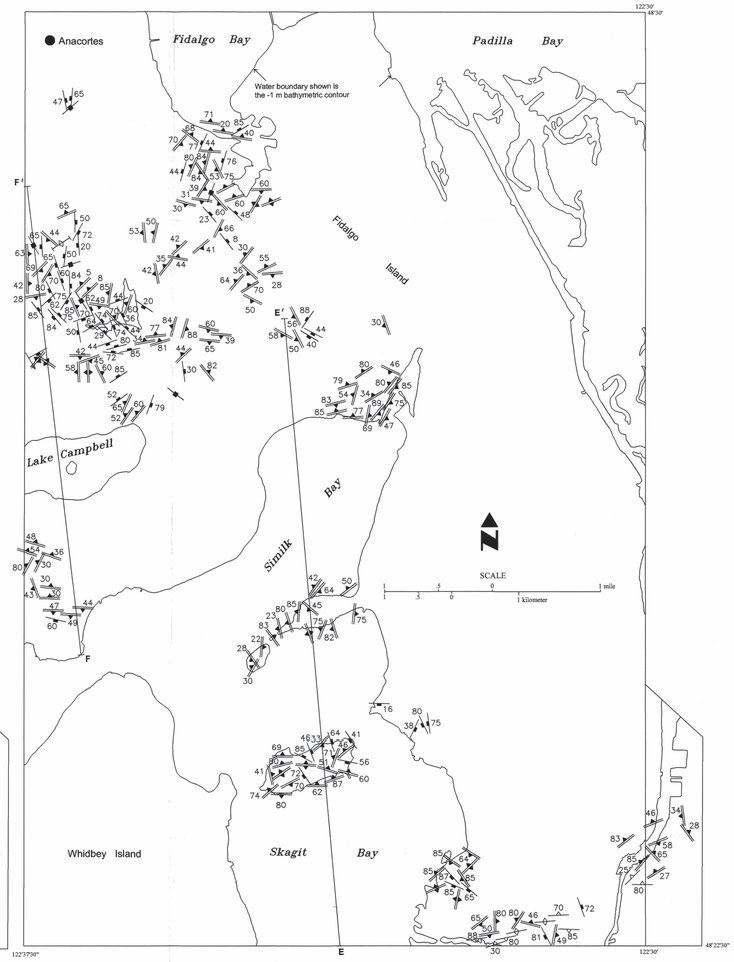

REFERENCES CITED

Armstrong, J. E.; Crandell, D. R.; Easterbrook, D. J.; Noble, J. B., 1965, Late Pleistocene stratigraphic chronology in southwestern British Columbia and northwestern Washington [abstract]: Geological Society of America Special Paper 82, p. 237.

Beget, J. E., 1981, Postglacial eruption history and volcanic hazards at Glacier Peak, Washington: University of Washington Doctor of Philosophy thesis, 192 p.

Beget, J. E., 1982, Postglacial volcanic deposits at Glacier Peak, Washington, and potential hazards from future eruptions: U.S. Geological Survey Open-File Report 82-830, 77 p.

Blakely, R. J.; Wells, R. E.; Weaver, C. S., 1999, Puget Sound aeromagnetic maps and data: U.S. Geological Survey Open-File Report 99-514, version 1.0 [accessed Oct. 3, 2000 at http://geopubs.wr.usgs.gov/open-file/of99-514/].

Borden, R. K.; Troost, K. G., in progress, Late Pleistocene stratigraphy in the south-central Puget Lowland, west-central Pierce County, Washington: Washington Division of Geology and Earth Resources Report of Investigations.

Brandon, M. T.; Cowan, D. S.; Vance, J. A., 1988, The Late Cretaceous San Juan thrust system, San Juan Islands, Washington: Geological Society of America Special Paper 221, 81 p., 1 pl.

Brown, E. H., 1977, Ophiolite on Fidalgo Island, Washington. *In* Coleman, R. G.; Irwin, W. P., editors, North American ophiolites: Oregon Department of Geology and Mineral Industries Bulletin 95, p. 67-73.

Brown, E. H.; Bradshaw, J. Y.; Mustoe, G. E., 1979, Plagiogranite and keratophyre in ophiolite on Fidalgo Island, Washington: Geological Society of America Bulletin, v. 90, no. 5, p. I 493-I 507.

Carroll, P. R., 1980, Petrology and structure of the pre-Tertiary rocks of Lummi and Eliza Islands, Washington: University of Washington Master of Science thesis, 78 p., 1 plate.

Clague, J. J.; Saunders, I. R.; Roberts, M. C., 1988, Ice-free conditions in southwestern British Columbia at 16,000 years BP: Canadian Journal of Earth Sciences, v. 25, no. 6, p. 938-941.

Deeter, J. D., 1979, Quaternary geology and stratigraphy of Kitsap County, Washington: Western Washington University Master of Science thesis, 175 p., 2 pl.

Dethier, D. P.; Whetten, J. T., 1981, Preliminary geologic map of the Mount Vernon 7.5-minute quadrangle, Skagit County, Washington: U.S. Geological Survey Open-File Report 81-105, 9 p., 1 pl.

Dethier, D. P.; White, D. P.; Brookfield, C. M., 1996, Maps of the surficial geology and depth to bedrock of False Bay, Friday Harbor, Richardson, and Shaw Island 7.5-minute quadrangles, San Juan County, Washington: Washington Division of Geology and Earth Resources Open File Report 96-7, 7 p., 2 pl.

Dragovich, J. D.; McKay, D. T., Jr.; Dethier, D. P.; Beget, J. E., 2000, Voluminous laharic inundation of the lower Skagit River valley, Washington--A product of a single large mid-Holocene Glacier Peak eruptive episode? [abstract]: Geological Society of America Abstracts with Programs, v. 32, no. 6, p. A-11.

Dragovich, J. D.; Norman, D. K.; Grisamer, C. L.; Logan, R. L.; Anderson, Garth, 1998, Geologic map and interpreted geologic history of the Bow and Alger 7.5-minute quadrangles, western Skagit County, Washington: Washington Division of Geology and Earth Resources Open File Report 98-5, 80 p., 3 pl.

Dragovich, J. D.; Norman, D. K.; Lapen, T. J.; Anderson, Garth, 1999, Geologic map of the Sedro-Woolley North and Lyman 7.5-minute quadrangles, western Skagit County, Washington: Washington Division of Geology and Earth Resources Open File Report 99-3, 37 p., 4 pl.

Easterbrook, D. J., 1962, Pleistocene geology of the northern part of the Puget Lowland, Washington: University of Washington Doctor of Philosophy thesis, 160 p.

Easterbrook, D. J., 1969, Pleistocene chronology of the Puget Lowland and San Juan Islands, Washington: Geological Society of America Bulletin, v. 80, no. 11, p. 2273-2286.

Easterbrook, D. J., 1971, Geology and geomorphology of western Whatcom County: Western Washington State College Department of Geology, 68 p.

Easterbrook, D. J., 1976a, Geologic map of western Whatcom County, Washington: U.S. Geological Survey Miscellaneous Investigations Series Map I-854-B, 1 sheet, scale 1:62,500.

Easterbrook, D. J., 1976b, Quaternary geology of the Pacific Northwest. *In* Mahaney, W. C., editor, Quaternary stratigraphy of North America: Dowden, Hutchinson and Ross, p. 441-462.

Easterbrook, D. J., 1994, Chronology of pre-late Wisconsin Pleistocene sediments in the Puget Lowland, Washington. *In* Lasmanis, Raymond; Cheney, E. S., convenors, Regional geology of Washington State: Washington Division of Geology and Earth Resources Bulletin 80, p. 191-206.

Easterbrook, D. J.; Rutter, N. W., 1981, Amino acid ages of Pleistocene glacial and interglacial sediments in western Washington [abstract]: Geological Society of America Abstracts with Programs, v. 13, no. 7, p. 444.

Easterbrook, D. J.; Rutter, N. W., 1982, Amino acid analyses of wood and shells in development of chronology and correlation of Pleistocene sediments in the Puget Lowland, Washington [abstract]: Geological Society of America Abstracts with Programs, v. 14, no. 7, p. 480.

Garver, J. I., 1988, Stratigraphy, depositional setting, and tectonic significance of the clastic cover to the Fidalgo ophiolite, San Juan Islands, Washington: Canadian Journal of Earth Sciences, v. 25, no. 3, p. 417-432.

Gusey, D. L., 1978, The geology of southwestern Fidalgo Island: Western Washington University Master of Science thesis, 85 p., 1 pl.

Hopkins, W. S., Jr., 1962, The geology of a portion of the Skagit delta area, Skagit County, Washington: University of British Columbia Master of Science thesis, 135 p., 1 pl.

Johnson, S. Y.; Dadisman, S. V.; Mosher, D. C.; Blakely, R. J.; Childs, J. R., 2000, Late Quaternary tectonics of the Devils Mountain fault and related structures, northern Puget Lowland [abstract]: Geological Society of America Abstracts with Programs, v. 32, no. 6, p. A-21 - A-22.

Johnson, S. Y.; Dadisman, S. V.; Mosher, D. C.; Blakely, R. J.; Childs, J. R., in progress, Active tectonics of the Devils Mountain fault and related structures, northern Puget Lowland and eastern Strait of Juan de Fuca region, Pacific Northwest: U.S. Geological Survey Professional Paper.

Johnson, S. Y.; Zimmermann, R. A.; Naeser, C. W., 1986, Fission-track dating of the tectonic development of the San Juan Islands, Washington: Canadian Journal of Earth Sciences, v. 23, no. 9, p. 1318-1330.

Misch, Peter, 1966, Tectonic evolution of the northern Cascades of Washington--A west-cordilleran case history. *In* Canadian Institute of Mining and Metallurgy; and others, A symposium on the tectonic history and mineral deposits of the western Cordillera in British Columbia and neighbouring parts of the United States, Vancouver, 1964: Canadian Institute of Mining and Metallurgy Special Volume 8, p. 101-148, 1 pl.

Mullineaux, D. R.; Waldron, H. H.; Rubin, Meyer, 1965, Stratigraphy and chronology of late interglacial and early Vashon glacial time in the Seattle area, Washington: U.S. Geological Survey Bulletin 1194-O, 10 p.

Pessl, Fred, Jr.; Dethier, D. P.; Booth, D. B.; Minard, J. P., 1989, Surficial geologic map of the Port Townsend 30- by 60-minute quadrangle, Puget Sound region, Washington: U.S. Geological Survey Miscellaneous Investigations Series Map I-1198-F, 1 sheet, scale 1:100,000, with 13 p. text.

Porter, S. C.; Swanson, T. W., 1998, Radiocarbon age constraints on rates of advance and retreat of the Puget Lobe of the Cordilleran ice sheet during the last glaciation: Quaternary Research, v. 50, no. 3, p. 205-213.

Siegfried, R. T., 1978, Stratigraphy and chronology of raised marine terraces, Bay View Ridge, Skagit County, Washington: Western Washington University Master of Science thesis, 52 p., 1 pl.

Stoffel, K. L., 1980, Stratigraphy of pre-Vashon Quaternary sediments applied to the evaluation of a proposed major tectonic structure in Island County, Washington: U.S. Geological Survey Open-File Report 81-292; Washington Division of Geology and Earth Resources Open File Report, 161 p.

Tabor, R. W., 1994, Late Mesozoic and possible early Tertiary accretion in western Washington State-The Helena-Haystack mélange and the Darrington-Devils Mountain fault zone: Geological Society of America Bulletin, v. 106, no. 2, p. 217-232, 1 pl.

Tabor, R. W.; Booth, D. B.; Vance, J. A.; Ford, A. B.; Ort, M. H., 1988, Preliminary geologic map of the Sauk River 30 by 60 minute quadrangle, Washington: U.S. Geological Survey Open-File Report 88-692, 50 p., 2 pl.

Tabor, R. W.; Crowder, D. F., 1969, On batholiths and volcanoes--Intrusion and eruption of late Cenozoic magmas in the Glacier Peak area, North Cascades, Washington: U.S. Geological Survey Professional Paper 604, 67 p., 1 pl.

Thompson, Gail, 1978, Prehistoric settlement changes in the southern northwest coast--A functional approach: University of Washington Doctor of Philosophy thesis, 251 p.

Whetten, J. T.; Carroll, P. I.; Gower, H. D.; Brown, E. H.; Pessl, Fred, Jr., 1988, Bedrock geologic map of the Port Townsend 30- by 60-minute quadrangle, Puget Sound region, Washington: U.S. Geological Survey Miscellaneous Investigations Series Map I-1198-G, 1 sheet, scale 1:100,000.

Whetten, J. T.; Jones, D. L.; Cowan, D. S.; Zartman, R. E., 1978, Ages of Mesozoic terranes in the San Juan Islands, Washington. *In* Howell, D. G.; McDougall, K. A., editors, Mesozoic paleogeography of the western United States: Society of Economic Paleontologists and Mineralogists Pacific Section, Pacific Coast Paleogeography Symposium 2, p. 117-132.

Whetten, J. T.; Zartman, R. E.; Blakely, R. J.; Jones, D. L., 1980, Allochthonous Jurassic ophiolite in northwest Washington: Geological Society of America Bulletin, v. 91, no. 6, p. I 359-I 368.